Physica D 467 (2024) 134262

Contents lists available at ScienceDirect

Physica D

journal homepage: www.elsevier.com/locate/physd

Darboux transformation-based LPNN generating novel localized wave solutions

Juncai Pu [a], Yong Chen [b,c,*]

[a] Institute of Applied Physics and Computational Mathematics, Beijing, 100088, China

[b] School of Mathematical Sciences, Key Laboratory of Mathematics and Engineering, Applications (Ministry of Education) & Shanghai Key Laboratory of PMMP, East China Normal University, Shanghai, 200241, China

[c] College of Mathematics and Systems Science, Shandong University of Science and Technology, Qingdao, 266590, China

ARTICLE INFO

Communicated by B. Hamzi

Keywords:
Darboux transformation-based LPNN
Localized wave solutions
Darboux transformation
Kraenkel–Manna–Merle system

ABSTRACT

Darboux transformation method is one of the most essential and important methods for solving localized wave solutions of integrable systems. In this work, we introduce the core idea of Darboux transformation of integrable systems into the Lax pairs informed neural networks (LPNNs), which we proposed earlier. By fully utilizing the data-driven solutions, spectral parameter and spectral function obtained from LPNNs, we present the novel Darboux transformation-based LPNN (DT-LPNN). The notable feature of DT-LPNN lies in its ability to solve data-driven localized wave solutions and spectral problems with high precision, and it also can employ Darboux transformation formulas of integrable systems and non-trivial seed solutions to discover novel localized wave solutions that were previously unobserved and unreported. The numerical results indicate that, by utilizing the single-soliton solutions as the non-trivial seed solutions, we obtain novel localized wave solutions for the Kraenkel–Manna–Merle (KMM) system by employing DT-LPNN, in which solution u changes from original bright single-soliton on zero background wave to new dark single-soliton dynamic behavior on a variable non-zero background wave. Moreover, by treating the two-soliton solutions as the non-trivial seed solutions, DT-LPNN generates novel localized wave solutions for the KMM system that exhibit completely different dynamic behaviors from prior two-soliton solutions. DT-LPNN combines the Darboux transformation theory of integrable systems with deep neural networks, offering a new approach for generating novel localized wave solutions using non-trivial seed solutions.

1. Introduction

The utilization of deep learning methods for solving nonlinear partial differential equations (PDEs) has emerged as a research hotspot in recent years, and many effective deep learning approaches have been proposed and successfully applied to efficiently solve a variety of PDEs in multiple research fields [1–8]. Integrable systems, as a special class of PDEs, play a crucial role in nonlinear science and mathematical physics [9]. The origin and development of integrable system theory are closely intertwined with the flourishing advancements in computer science [10]. The resurgence of deep learning in recent years is considered a significant breakthrough in the field of computer science [11, 12]. Consequently, investigating various problems related to integrable systems using deep learning methods represents a cutting-edge research area.

In 2019, inspired by the physics-informed neural network (PINN) algorithm proposed by Kaniadakis [1], Chen's research team begin explored the application of deep learning methods in the study of integrable systems [13]. Subsequently, they proposed the establishment of a unified framework for integrable deep learning and dedicated efforts to the research of efficient algorithms for integrable deep learning. As of now, Chen's research group has achieved numerous significant research outcomes. Specifically, utilizing the PINN algorithm and its various improved versions, they have successfully learned various high precision data-driven localized wave solutions, including various rogue waves [14], rogue waves on periodic background waves [15] and interaction solutions [16] and so on. Additionally, they have investigated forward-inverse problems of various integrable models, such as coupled integrable systems [17], nonlocal integrable systems [18], high-dimensional integrable systems [19] and variable coefficient integrable systems [20]. Furthermore, other research groups have also made excellent research work in the integrable deep learning field, such as learning data-driven peakon solutions with discontinuous first-order

* Corresponding author at: School of Mathematical Sciences, Key Laboratory of Mathematics and Engineering, Applications (Ministry of Education) & Shanghai Key Laboratory of PMMP, East China Normal University, Shanghai, 200241, China.

E-mail address: ychen@sei.ecnu.edu.cn (Y. Chen).

https://doi.org/10.1016/j.physd.2024.134262
Received 30 January 2024; Received in revised form 22 April 2024; Accepted 12 June 2024
Available online 15 June 2024

derivative at the wave peak [21], studying nearly integrable systems with various $\mathcal{PT}$-symmetric potentials [22,23], and proposing the two-stage initial-value iterative neural network to simulate different types nonlinear solutions [24], we refer the reader to Refs. [25–30] for more work. Importantly, the significant features and theoretical methods of integrable systems have been integrated with deep learning approaches, then obtained outstanding research outcomes, including the infinite conservation law [31], Miura transformation [32] and Bäcklund transformation [25]. Prior to this, we successfully incorporated the most crucial characteristic of integrable systems, namely Lax pairs, into deep learning method and proposed a Lax pairs informed neural networks (LPNNs) capable of efficiently and accurately solving integrable systems with Lax pairs [33]. Therefore, the inspiration of this article stems from how to make full utilize of the data-driven spectral parameter and spectral function obtained from the LPNNs.

The Darboux transformation is one of the most important methods for systematically solving exact solutions to integrable systems [34]. It starts directly from the Lax pairs of integrable systems and obtains new Lax pairs with the same form by constructing appropriate gauge transformation to act on the original Lax pairs. Thereby one can obtain the iterative relationship between the new and old spectral functions and the new and old solutions, and iterate a series of new solutions in sequence. In 1882, the approach provided by Darboux in dealing with the spectral problem of the second-order ordinary differential Sturm–Liouville equation was proven to play a vital role in the explicit solution of PDEs [35], which is also considered the origin of Darboux transformation theory. For second-order differential equation

$$\psi_{xx} - u\psi = \lambda\psi, \tag{1.1}$$

under the transformation

$$\begin{cases} \hat{\psi} = \psi_x - \dfrac{\psi_{1,x}}{\psi_1}\psi \\ \hat{u} = u - 2(\ln\psi_1)_{xx} \end{cases} \tag{1.2}$$

is invariant, namely $\hat{\psi}$, $\hat{u}$ satisfy the same form as Eq. (1.1), as shown bellow

$$\hat{\psi}_{xx} - \hat{u}\hat{\psi} = \lambda\hat{\psi},$$

in which ψ_1 is a particular solution of Eq. (1.1) as parameter $\lambda = \lambda_1$, we call transformation (1.2) as Darboux transformation of second-order differential equation. More generally, second-order differential equation (1.1) usually correspond to the spatial part of the Lax pairs for classical integrable systems, if the transformation (1.2) simultaneously takes into account the temporal part of the Lax pairs, thus the Darboux transformations of the integrable systems are obtained. It starts from the old solution [also be called seed solution] u and iteratively constructs new solution $\hat{u}$ of the integrable system, for a more detailed introduction, we refer the reader to Ref. [34]. In Ref. [33], we can know that LPNNs can efficiently solve integrable systems with Lax pairs, and obtain abundant data-driven localized wave solutions, spectral parameter and corresponding spectral function. Generally, the Darboux transformations of integrable systems involve both old and new solutions, spectral parameter and corresponding spectral function in Lax pairs, as shown in Eq. (1.2). Fortunately, the aforementioned quantities can all be obtained utilizing LPNNs, hence introducing the Darboux transformation into LPNNs is a natural and feasible idea.

Solving localized wave solutions for nonlinear integrable systems is a research focus in integrable system theory. Common localized wave solutions include soliton solution, breather solution, rogue wave solution, peak solution, lump solution and mixed interaction solution, among others [10,36–39]. The commonly used methods for solving nonlinear integrable systems contain inverse scatting transformation method [40], Hirota bilinear method [41], Bäcklund transformation method [42] and Darboux transformation method [34] and so on. However, these methods usually only yield common localized wave solutions. In recent years, the utilize of various solving methods to generate novel localized wave solutions has become a research hotspot. As is well known, as long as there are enough layers and neurons in the network, deep neural networks (NNs) can learn any Borel measurable functions due to their powerful approximation ability [43]. Moreover, many important transformations in the integrable system theory are particularly suitable for constructing relationships between new and known solutions, such as the Mirua transformation [44], Bäcklund transformation, and Darboux transformation. Significantly, Ref. [32] provided a possibility for new types of numerical solutions by fully leveraging the many-to-one relationship between solutions before and after Miura transformation, and offered a new approach for constructing new localized wave solutions by combining NNs and integrable system theory. Therefore, it is an important research direction to generate novel localized wave solutions by combine the emerging deep NNs with various transformations in the integrable system theory.

In this work, we cleverly incorporate the Darboux transformation theory into LPNNs, then propose a Darboux transformation-based LPNN (DT-LPNN), and utilize non-trivial seed solutions to construct novel localized wave solutions for integrable systems. The main highlights of this article are: In order to harness the spectral parameter and spectral function learned in previous LPNNs, we incorporate the Darboux transformation theory into LPNNs, resulting in the DT-LPNN. This enhanced model not only solves localized wave solutions and spectral problems with high-accuracy, but also has the capability to discover novel localized wave solutions by means of non-trivial seed solutions. We numerically generate two previously unreported and unobserved localized wave solutions for the Kraenkel–Manna–Merle (KMM) system by means of the DT-LPNN, particularly the dark soliton solution u on a variable non-zero background wave, which is a very important discovery.

The paper's organization is as follows: Section 2 introduces the Darboux transformation of integrable systems and innovative DT-LPNN model. In Section 3, we present a comprehensive display of numerical experiments conducted to validate the effectiveness of our proposed DT-LPNN method. Section 4 encapsulates our work and draws meaningful conclusions from the outcomes.

2. Methodology

Generally, we consider a multi-dimensional spatiotemporal real nonlinear integrable system with operator Lax pairs f_{oLp} or matrix Lax pairs f_{mLp} in the general form given by

$$\mathcal{F}[\boldsymbol{q}, \boldsymbol{q}^2, \ldots, \nabla_t \boldsymbol{q}, \nabla_t^2 \boldsymbol{q}, \ldots, \nabla_{\mathbf{x}} \boldsymbol{q}, \nabla_{\mathbf{x}}^2 \boldsymbol{q}, \ldots, \boldsymbol{q}\cdot\nabla_t \boldsymbol{q}, \ldots, \boldsymbol{q}\cdot\nabla_{\mathbf{x}} \boldsymbol{q}, \ldots] = 0, \tag{2.1a}$$

$$f_{\mathrm{oLp}}: \begin{cases} L\psi = \lambda\psi \\ \psi_t = A\psi \end{cases}, \text{ usually for } \mathbf{x}\in\Omega, \text{ or}$$
$$f_{\mathrm{mLp}}: \begin{cases} \Psi_x = M\Psi \\ \Psi_t = N\Psi \end{cases}, \text{ usually for } \mathbf{x} = x, \tag{2.1b}$$

in which potential $\boldsymbol{q} = \boldsymbol{q}(\mathbf{x}, t) \in \mathbb{R}^{n\times 1}$ is the n-dimensional latent solution, $\mathbf{x} \in \Omega$ specifies the n-dimensional space and $t \in [S_{\mathrm{i}}, S_{\mathrm{f}}]$ denotes time [S_{i} and S_{f} respectively indicate the initial time and final time], $\mathcal{F}[\cdot]$ is a complex nonlinear operator of $\boldsymbol{q}$ and its spatiotemporal derivatives, ∇ is the gradient operator with respect to $\mathbf{x}$ and t. Here linear operator L involves space $\mathbf{x}$ and potential $\boldsymbol{q}$, λ indicates spectral parameter and ψ represents spectral function corresponding to spectral parameter. $\Psi = \Psi(\mathbf{x}, t)$ stands for vector spectral function corresponding to spectral parameter λ in matrices M and N. In general, low-dimensional integrable systems can be represented using the operator Lax pairs or matrix Lax pairs, while high-dimensional integrable systems are typically expressed using the operator Lax pairs, this also explains why the spatial variable of the matrix Lax pairs f_{mLp} in Eq. (2.1b) is $\mathbf{x} = x$ [namely one-dimensional space]. Specific examples can refer to Ref. [33].

Usually, from Lax pairs (2.1b), we can derive all integrable systems by means of the following compatibility condition equation f_{cce} [for Lax pairs of operator form] and zero curvature equation f_{zce} [for Lax pairs of matrix form], that is

$$f_{\text{cce}}: \psi_{\underbrace{\mathbf{x}\cdots\mathbf{x}}_{\forall h,\, h\geq 1}\, t} - \psi_{t\,\underbrace{\mathbf{x}\cdots\mathbf{x}}_{\forall h,\, h\geq 1}} = 0, \tag{2.2}$$

and

$$f_{\text{zce}}: M_t - N_x + [M, N] = 0, \tag{2.3}$$

where $h \geq 1$ is a finite positive integer, and the size of h is determined by the dimensions of space $\mathbf{x}$ and the form of Lax pairs spatial part, $\psi_{\mathbf{x}\cdots\mathbf{x}}$ indicates ψ taking hth partial derivative of space $\mathbf{x}$. In fact, $\psi_{\mathbf{x}\cdots\mathbf{x}\,t}$ is obtained by taking partial derivative of t on both sides of the first equation [namely $L\psi = \lambda\psi$, here the specific form of L has been known] of operator Lax pairs f_{oLp} in Eq. (2.1b), and $\psi_{t\,\mathbf{x}\cdots\mathbf{x}}$ is obtained by taking the h-order partial derivative of $\mathbf{x}$ on both sides of the second equation [namely $\psi_t = A\psi$, here the specific form of A has been known] of operator Lax pairs f_{oLp} in Eq. (2.1b).

Then we consider the initial and boundary conditions of spatiotemporal nonlinear integrable system denoted by

$$\begin{aligned} &\mathcal{I}[\boldsymbol{q}, \psi/\Psi; \mathbf{x} \in \Omega, t = S_{\text{i}}] = 0, \\ &\mathcal{B}[\boldsymbol{q}, \psi/\Psi, \nabla_{\mathbf{x}}\boldsymbol{q}; \mathbf{x} \in \partial\Omega, t \in [S_{\text{i}}, S_{\text{f}}]] = 0. \end{aligned} \tag{2.4}$$

Here $\partial\Omega$ indicates boundary of Ω. If we consider a complex valued potential $\tilde{\boldsymbol{q}} \in \mathbb{C}^{n\times 1}$ for nonlinear integrable system, we can utilize decomposition $\tilde{\boldsymbol{q}} = \tilde{\boldsymbol{u}} + \mathrm{i}\tilde{\boldsymbol{v}}$ to derive two real-value functions $\tilde{\boldsymbol{u}} \in \mathbb{R}^{n\times 1}$ and $\tilde{\boldsymbol{v}} \in \mathbb{R}^{n\times 1}$, then back to the problem of Eq. (2.1a). The initial and boundary points set $\mathcal{D}_{\text{ib}}$ for training is sampled randomly via corresponding initial and boundary conditions (2.4), and the collocation points set $\mathcal{D}_{\text{c}}$ for training is generated by means of the Latin Hypercube Sampling method [45].

2.1. Darboux transformation of integrable systems with Lax pairs

The Darboux transformation method stands as a theoretical approach employed to exactly solve integrable systems with Lax pairs, holding a significant role in the landscape of integrable system theory [34]. The core concept of Darboux transformation is to construct new exact solutions using known exact solutions, which is essentially a special gauge transformation. Starting from the Lax pairs of integrable system, the Darboux transformation can be directly obtained, which can usually be iterated sequentially to obtain the relationship between multiple new solutions and seed solutions. Usually, after determining the spectral parameter of Lax pairs, the seed solution is usually chosen as either a trivial solution or a plane wave solution, which can easily solve the spectral function and then iteratively construct a new solution. In this part, for generating novel localized wave solutions of integrable systems via deep learning method, we combine the Darboux transformation method with the powerful solving ability of localized wave solutions and spectral problems in LPNNs, to construct novel localized wave solutions via non-trivial seed solutions.

Next, we assume that the integrable system (2.1) with Lax pairs possesses the 1-fold operator Darboux transformation $D^{[1]}$ or matrix Darboux transformation $T^{[1]}$, which satisfy

$$\psi^{[1]} = D^{[1]}\psi, \text{ or } \Psi^{[1]} = T^{[1]}\Psi. \tag{2.5}$$

Then $\psi^{[1]}$ and $\Psi^{[1]}$ satisfy new operator Lax pairs f_{noLp} or new matrix Lax pairs f_{nmLp}, as shown bellow

$$\begin{aligned} &f_{\text{noLp}}: \begin{cases} L^{[1]}\psi^{[1]} = \lambda\psi^{[1]} \\ \psi_t^{[1]} = A^{[1]}\psi^{[1]} \end{cases}, \text{ usually for } \mathbf{x} \in \Omega, \text{ or} \\ &f_{\text{nmLp}}: \begin{cases} \Psi_x^{[1]} = M^{[1]}\Psi^{[1]} \\ \Psi_t^{[1]} = N^{[1]}\Psi^{[1]} \end{cases}, \text{ usually for } \mathbf{x} = x, \end{aligned} \tag{2.6}$$

where the form of the new Lax pairs (2.6) is consistent with that of Lax pairs (2.1b). Here operators $L^{[1]}$ and $A^{[1]}$, matrixes $M^{[1]}$ and $N^{[1]}$ involve new potential function $\boldsymbol{q}_{\text{new}}$ of integrable system, which satisfies

$$\begin{aligned} &\mathcal{F}[\boldsymbol{q}_{\text{new}}, \boldsymbol{q}_{\text{new}}^2, \ldots, \nabla_t\boldsymbol{q}_{\text{new}}, \nabla_t^2\boldsymbol{q}_{\text{new}}, \ldots, \nabla_{\mathbf{x}}\boldsymbol{q}_{\text{new}}, \\ &\quad \nabla_{\mathbf{x}}^2\boldsymbol{q}_{\text{new}}, \ldots, \boldsymbol{q}_{\text{new}} \cdot \nabla_t\boldsymbol{q}_{\text{new}}, \ldots, \boldsymbol{q}_{\text{new}} \cdot \nabla_{\mathbf{x}}\boldsymbol{q}_{\text{new}}, \ldots] = 0, \end{aligned}$$

in which the form of nonlinear operator $\mathcal{F}$ here is the same as that of nonlinear operator $\mathcal{F}$ in Eq. (2.1a). Subsequently, with the help of Darboux transformation theory and symbolic calculation, we can derive Darboux transformation related to the particular solution of Lax pairs, and obtain the following 1-fold Darboux transformation theorem between new and seed solutions:

Theorem 2.1. *The integrable system (2.1) has the Darboux transformation formula of new solution*

$$\boldsymbol{q}_{\text{new}} = \boldsymbol{q}_{\text{seed}} + \boldsymbol{\Gamma}(\mathbf{x}, t, \psi_{\text{s}}/\Psi_{\text{s}}, \lambda_1), \tag{2.7}$$

in which $\boldsymbol{q}_{\text{seed}}$ satisfies the Lax pairs (2.1b), while $\boldsymbol{q}_{\text{new}}$ satisfies the Lax pairs (2.6) after Darboux transformation (2.5), they both are solutions of integrable system (2.1a). Moreover, $\boldsymbol{\Gamma} \in \mathbb{R}^{n\times 1}$ is an arbitrary function that is only related to space $\mathbf{x}$, time t, spectral parameter λ_1 and spectral function $\psi_{\text{s}}/\Psi_{\text{s}}$, while spectral functions ψ_s and Ψ_s are the particular solutions obtained from the Lax equations (2.1b) when the spectral parameter $\lambda = \lambda_1$ and the seed solution $\boldsymbol{q} = \boldsymbol{q}_{\text{seed}}$.

Generally, if we take a trivial seed solution $\boldsymbol{q}_{\text{seed}} = \mathbf{0}$, then we can obtain the exact 1-soliton solution $\boldsymbol{q}_{\text{new}}$ of the integrable system (2.1a) by means of 1-fold Darboux transformation (2.7). Correspondingly, if we further construct the N-fold operator Darboux transformation $D^{[N]}$ or matrix Darboux transformation $T^{[N]}$ [here $N \geq 2$ is a positive integer], then one can obtain N-soliton solution of integrable system (2.1a). For more details, we refer the reader to Ref. [34].

However, once we consider non-trivial seed solution $\boldsymbol{q}_{\text{seed}}$, it becomes very difficult for solving spectral problem (2.1b). From Ref. [33], by designing novel network architectures and loss functions, we proposed the LPNNs tailored for the integrable systems with Lax pairs, including LPNN-v1 and LPNN-v2. The most noteworthy advantage of LPNN-v1 is that it can transform the solving of nonlinear integrable systems into the solving of relatively simpler Lax pairs, and it not only efficiently solves data-driven localized wave solutions, but also obtains spectral parameter and corresponding spectral function in Lax pairs of integrable systems. On the basis of LPNN-v1, we additionally incorporate the compatibility condition/zero curvature equation of Lax pairs in LPNN-v2, its major advantage is the ability to solve and explore high-accuracy data-driven localized wave solutions and associated spectral problems for integrable systems with Lax pairs. That is to say, if we use non-trivial seed solutions as the training target, LPNNs cannot only obtain high-precision non-trivial seed solutions, but also obtain the corresponding spectral parameter and spectral function of spectral problem, which is exactly the data required for our new solutions' Darboux transformation (2.7). Therefore, we can utilize the output of LPNNs and Darboux transformation formula to construct novel localized wave solutions for integrable system (2.1).

2.2. Darboux transformation-based LPNN

Based on the LPNNs in Ref. [33] and Darboux transformation Theorem 2.1 of new solution for integrable system, we present the DT-LPNN, Fig. 1 displays schematic architecture of the DT-LPNN model for integrable system.

Different from the LPNNs, in Fig. 1**a**, except for the NN part of left panel and the Lax pairs informed part of right panel, the middle panel also includes the Darboux transformation part with spectral parameter λ. In the left panel of Fig. 1**a**, we employ a standard fully connected NN, with input layer contains $\mathbf{x}$ and t, and output layer contains the seed solution of integrable system and the spectral function of the Lax pairs.

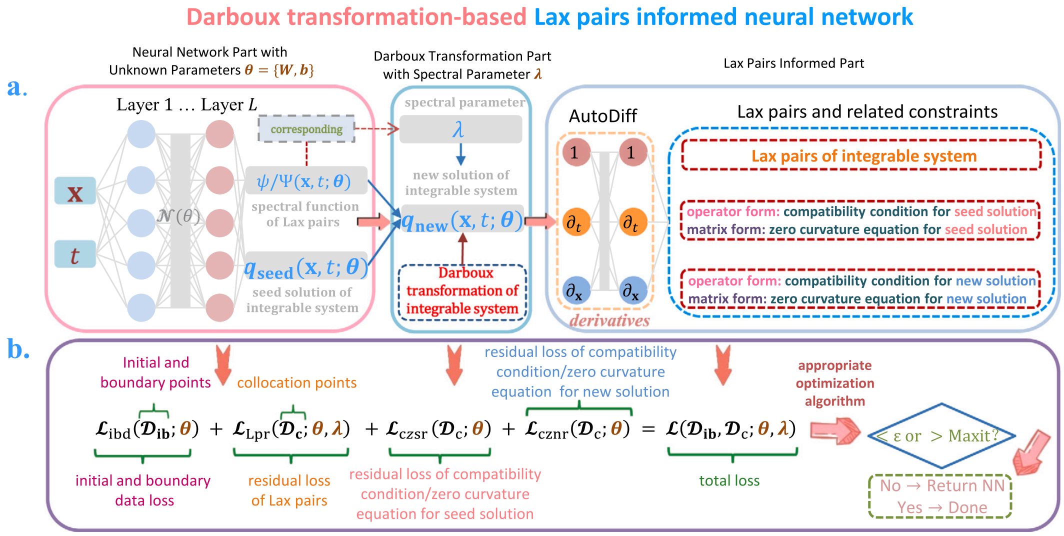

Fig. 1. Schematic architecture of the DT-LPNN model for integrable system. **a**. The NN part (left panel), Darboux transformation part (middle panel), and Lax pairs informed part (right panel). **b**. The components of the loss function and optimize process in DT-LPNN.

From the Darboux transformation part of middle panel in Fig. 1**a**, a new solution $\boldsymbol{q}_{\text{new}}$ is yielded by employing the Darboux transformation of integrable system, where the Darboux transformation formula usually involves the seed solution $\boldsymbol{q}_{\text{seed}}$, spectral parameter λ and corresponding particular solution ψ_s/Ψ_s of spectral function. Furthermore, in the Lax pairs informed part of Fig. 1**a** right panel, the Lax pairs and their related constraints are also completely different from LPNNs in Ref. [33], as they consist of three parts: Lax pairs of integrable system, compatibility condition/zero curvature equation for seed solution, and compatibility condition/zero curvature equation for new solution. Correspondingly, lower panel **b** of Fig. 1 exhibits different composition of loss function, then novel total loss function is defined as

$$\mathcal{L}(\mathcal{D}_{\text{ib}},\mathcal{D}_{\text{c}};\boldsymbol{\theta},\lambda)=\mathcal{L}_{\text{ibd}}(\mathcal{D}_{\text{ib}};\boldsymbol{\theta})+\mathcal{L}_{\text{Lpr}}(\mathcal{D}_{\text{c}};\boldsymbol{\theta},\lambda)+\mathcal{L}_{\text{czsr}}(\mathcal{D}_{\text{c}};\boldsymbol{\theta})+\mathcal{L}_{\text{cznr}}(\mathcal{D}_{\text{c}};\boldsymbol{\theta}). \tag{2.8}$$

Here, $\mathcal{L}_{\text{ibd}}$ represents the initial and boundary data loss, $\mathcal{L}_{\text{Lpr}}$ indicates residual loss of Lax pairs, they can be defined as following

$$\mathcal{L}_{\text{ibd}}(\mathcal{D}_{\text{ib}};\boldsymbol{\theta})=\frac{1}{N_{\text{ib}}}\left\|\boldsymbol{q}^{\boldsymbol{\theta},\text{ib}}_{\text{seed}}-\boldsymbol{q}^{\boldsymbol{m},\text{ib}}_{\text{seed}}\right\|_2^2, \tag{2.9}$$

$$\mathcal{L}_{\text{Lpr}}(\mathcal{D}_{\text{c}};\boldsymbol{\theta},\lambda)=\frac{1}{N_{\text{c}}}\left\|f^{\text{c}}_{\text{oLp}}/f^{\text{c}}_{\text{mLp}}\right\|_2^2, \tag{2.10}$$

where N_{ib} and N_{c} represent respectively the number of elements in sets $\mathcal{D}_{\text{ib}}$ and $\mathcal{D}_{\text{c}}$, $\|\cdot\|_2$ denotes the L^2 norm. Then $\boldsymbol{q}^{\boldsymbol{\theta},\text{ib}}_{\text{seed}}$ represents the learning results of $\boldsymbol{q}^{\boldsymbol{\theta}}_{\text{seed}}$ acting on initial and boundary points set $\mathcal{D}_{\text{ib}}$. Besides, $\boldsymbol{q}^{\boldsymbol{m},\text{ib}}_{\text{seed}}$ represents the measurement data of $\boldsymbol{q}_{\text{seed}}$ on initial and boundary points set $\mathcal{D}_{\text{ib}}$. The $f^{\text{c}}_{\text{oLp}}$ [or $f^{\text{c}}_{\text{mLp}}$] is value of operator Lax pairs f_{oLp} [or matrix Lax pairs f_{mLp}] on collocation points set $\mathcal{D}_{\text{c}}$. The $\mathcal{L}_{\text{czsr}}$ and $\mathcal{L}_{\text{cznr}}$ respectively represent the residual loss for compatibility condition/zero curvature equation of seed solution $\boldsymbol{q}_{\text{seed}}$ and the residual loss of compatibility condition/zero curvature equation of new solution $\boldsymbol{q}_{\text{new}}$, as following

$$\mathcal{L}_{\text{czsr}}(\mathcal{D}_{\text{c}};\boldsymbol{\theta})=\frac{1}{N_{\text{c}}}\left\|\{f_{\text{cce}}/f_{\text{zce}}\}^{\text{c}}_{\boldsymbol{q}_{\text{seed}}}\right\|_2^2, \tag{2.11}$$

$$\mathcal{L}_{\text{cznr}}(\mathcal{D}_{\text{c}};\boldsymbol{\theta})=\frac{1}{N_{\text{c}}}\left\|\{f_{\text{cce}}/f_{\text{zce}}\}^{\text{c}}_{\boldsymbol{q}_{\text{new}}}\right\|_2^2, \tag{2.12}$$

similarly, the $\{f_{\text{cce}}/f_{\text{zce}}\}^{\text{c}}_{\boldsymbol{q}_{\text{seed}}}$ is value of compatibility condition/zero curvature equation for seed solution on collocation points $\mathcal{D}_{\text{c}}$, while the other is value of compatibility condition/zero curvature equation for new solution on collocation points $\mathcal{D}_{\text{c}}$. From the loss function (2.8), one can observe that although the new solution does not have corresponding initial and boundary condition constraints, but it is required to satisfy the corresponding compatibility condition/zero curvature equation and is forcibly added to the loss function, which will ensure that the new solution generated from DT-LPNN satisfies the integrable system under study. We introduce the Darboux transformation method of integrable system into deep NN and construct a new loss function to propose the DT-LPNN model that can generate novel localized wave solutions. Ultimately, we display the primary steps of DT-LPNN in Algorithm 2.2.

Algorithm 2.2: The Darboux transformation-based LPNN for integrable system.

Step 1: Specification of training set in computational domain: *initial and boundary training points*: $\mathcal{D}_{\text{ib}}$, *Residual collocation training points*: $\mathcal{D}_{\text{c}}$.

Step 2: Derive the Darboux transformation formula for the relationship between new solution and seed solution via Darboux transformation theory of integrable system with Lax pairs.

Step 3: Construct NN output [including spectral function ψ/Ψ, seed solution $\boldsymbol{q}_{\text{seed}}$] with random initialization of parameter $\boldsymbol{\theta}$.

Step 4: Employ aforementioned Darboux transformation formula to construct Darboux transformation part, and obtain new solution $\boldsymbol{q}_{\text{new}}$ via the seed solution $\boldsymbol{q}_{\text{seed}}$, spectral parameter λ and corresponding particular solution of spectral function ψ/Ψ.

Step 5: Construct the Lax pairs informed part by substituting NN output and new solution $\boldsymbol{q}_{\text{new}}$ into the Lax pairs of integrable system, compatibility condition equation [operator form]/zero curvature equation [matrix form] for seed solution and new solution.

Step 6: Specification of the total loss function $\mathcal{L}(\mathcal{D}_{\text{ib}},\mathcal{D}_{\text{c}};\boldsymbol{\theta},\lambda)$.

Step 7: Seek the optimal parameters $\boldsymbol{\theta}^*$ using appropriate optimization algorithms for minimizing the total loss function $\mathcal{L}$ as

$$\boldsymbol{\theta}^*=\underset{\boldsymbol{\theta}\in\mathcal{N}}{\arg\min}\,\mathcal{L}(\mathcal{D}_{\text{ib}},\mathcal{D}_{\text{c}};\boldsymbol{\theta},\lambda).$$

---

3. Numerical experiment

In this section, we utilize DT-LPNN to study data-driven seed solutions, solve spectral problem and discover new localized wave solutions for integrable system with Lax pairs, then provide detailed numerical results and related dynamic behavior figures, and compare them with other deep learning methods. Uniformly, the DT-LPNN presented in this paper is implemented in Python based on the TensorFlow library.

All deep learning methods involved in this work (including PINN, LPNNS and DT-LPNN) adopt the hyperbolic tangent function (tanh) as the activation function and both possess 5 hidden-layer NNs with 100 neurons per hidden layer, namely $L = 5$ in Fig. 1.

As one of the most important theoretical methods for integrable systems, the Darboux transformation iteratively constructs nonlinear localized wave solutions starting from the seed solution of Lax pairs, which can systematically provide a series of accurate solutions for integrable systems. Its core idea is to find the gauge transformation formula for Lax pairs and the relationship between the new and seed solution of integrable system. Based on the LPNNs in Ref. [33], we introduce the Darboux transformation and propose novel DT-LPNN algorithm that can effectively construct new solutions of integrable system. The specific operations are as follows:

1. For the integrable system with Lax pairs studied, we obtain corresponding Darboux transformation formula between new and seed solution.

2. We use non-trivial seed solution as input data for training in the NN part of DT-LPNN to learn seed solution and spectral function.

3. We embed the corresponding Darboux transformation formula in the Darboux transformation part of DT-LPNN to obtain new localized wave solution based on the network output and corresponding spectral parameter.

4. In the Lax pairs informed part of DT-LPNN, except for the conventional constraints in the loss function of LPNNs, it is also necessary to force the new solution to satisfy the compatibility condition/zero curvature equation of the Lax pairs, thereby ensuring the reliability of the new solution.

Next, we exhibit a detailed example of applying DT-LPNN to construct new localized wave solutions for integrable system.

3.1. Darboux transformation of Kraenkel–Manna–Merle system

In order to describe the propagation of nonlinear electromagnetic short-waves in a saturated ferrite only in the x-direction perpendicular to the external saturating magnetic field, Kraenkel et al. constructed the KMM system [46]. Subsequently, by introducing a blend of coordinate transformations and expansion series of the magnetization density, Nguepjouo et al. have transformed the KMM system into the nonlinear evolution system [47], as shown below

$$\begin{aligned} &u_{xt} - u v_x + \kappa v_x = 0,\\ &v_{xt} + u u_x = 0, \end{aligned} \tag{3.1}$$

here the quantities $u(x,t)$ and $v(x,t)$ represent the magnetization density and the magnetic induction respectively. The parameter κ stands for the contribution of damping effects. After that, Kuetche et al. investigated an existing prolongation structure of the coupled system (3.1) resorting to its soliton structure, then extended the previous existing prolongation structure of the system while generating its higher-dimensional generalization associated to its general Lax pairs, then showed the system is integrable under the zero damping effect condition ($\kappa = 0$) [48], opening the way in looking for its localized wave solutions via the inverse scattering transformation method and Darboux transformation method [49,50]. The associated Lax pairs have therefore been provided, having as expression

$$f_{\mathrm{mLp}} : \begin{cases} \Psi_x = M\Psi \\ \Psi_t = N\Psi \end{cases}, \; M = \begin{bmatrix} \lambda v_x & \lambda u_x \\ \lambda u_x & -\lambda v_x \end{bmatrix}, \; N = \begin{bmatrix} \frac{1}{4\lambda} & -\frac{1}{2}u \\ \frac{1}{2}u & -\frac{1}{4\lambda} \end{bmatrix}. \tag{3.2}$$

We can directly derive the KMM system (3.1) with $\kappa = 0$ using the zero curvature equation (2.3) and corresponding Lax pairs (3.2). Especially, we set spectral function $\Psi(x,t) \in \mathbb{R}^{2\times 1}$ and spectral parameter $\lambda \in \mathbb{R}$, thus we take $\Psi(x,t) = (\psi_1(x,t), \psi_2(x,t))^{\mathrm{T}}$, where $\psi_j(x,t) \in \mathbb{R}^{1\times 1} [j = 1,2]$. Actually, we can also generalize the spectral function and spectral parameter to $\Psi \in \mathbb{C}^{2\times 1}, \lambda \in \mathbb{C}$, but in practical operation, we found that the training effect is better in the aforementioned special situation.

From Ref. [50], one can obtain the 1-fold Darboux transformation and single-soliton solutions. Specifically, the 1-fold matrix Darboux transformation $T^{[1]}$ of Lax pairs (3.2) for KMM system can be defined as

$$\Psi^{[1]} = T^{[1]}\Psi, \tag{3.3}$$

here $\Psi^{[1]}$ satisfies

$$\begin{aligned} &\begin{cases} \Psi^{[1]}_x = M^{[1]}\Psi^{[1]} \\ \Psi^{[1]}_t = N^{[1]}\Psi^{[1]} \end{cases}, \; M^{[1]} = \begin{bmatrix} \lambda v_{\mathrm{new},x} & \lambda u_{\mathrm{new},x} \\ \lambda u_{\mathrm{new},x} & -\lambda v_{\mathrm{new},x} \end{bmatrix}, \\ &N^{[1]} = \begin{bmatrix} \frac{1}{4\lambda} & -\frac{1}{2}u_{\mathrm{new}} \\ \frac{1}{2}u_{\mathrm{new}} & -\frac{1}{4\lambda} \end{bmatrix}. \end{aligned} \tag{3.4}$$

From Eqs. (3.3)–(3.4), one can derive

$$T^{[1]}_x = M^{[1]}T^{[1]} - T^{[1]}M, \; T^{[1]}_t = N^{[1]}T^{[1]} - T^{[1]}N.$$

Then one can deduce the gauge transformation as

$$T^{[1]} = I + \lambda R^{[1]}, \; R^{[1]} = \begin{bmatrix} r^{[1]}_{11} & r^{[1]}_{12} \\ r^{[1]}_{12} & -r^{[1]}_{11} \end{bmatrix},$$

where I is identity matrix, and let $T^{[1]}\Big|_{\lambda=\lambda_1} \begin{bmatrix} \psi_1 \\ \psi_2 \end{bmatrix} = 0$, one can obtain

$$r^{[1]}_{11} = \frac{\psi_2^2 - \psi_1^2}{\lambda_1(\psi_1^2 + \psi_2^2)}, \; r^{[1]}_{12} = \frac{-2\psi_1\psi_2}{\lambda_1(\psi_1^2 + \psi_2^2)}.$$

The iterative relationship between the new and seed solution can be obtained, as shown in the following theorem.

Theorem 3.1. *The KMM system (3.1) has the Darboux transformation formulas of new solutions*

$$u_{\mathrm{new}} = u_{\mathrm{seed}} - \frac{2\psi_1\psi_2}{\lambda_1(\psi_1^2 + \psi_2^2)}, \tag{3.5}$$

$$v_{\mathrm{new}} = v_{\mathrm{seed}} + \frac{\psi_2^2 - \psi_1^2}{\lambda_1(\psi_1^2 + \psi_2^2)} + g_1(t), \tag{3.6}$$

in which u_{seed} and v_{seed} satisfy the Lax pairs (3.2), while u_{new} and v_{new} satisfy the Lax pairs (3.4) after Darboux transformation (3.3), they both are solutions of KMM system (3.1).

Particularly, if we choose trivial seed solutions to the KMM system (3.1) as follows

$$u_{\mathrm{seed}} = 0, \tag{3.7}$$

$$v_{\mathrm{seed}} = \alpha x. \tag{3.8}$$

Thereby, we are able to directly obtain the spectral function of the Lax pairs (3.2) under the trivial seed solution (3.7)–(3.8) responding to $\lambda = \lambda_1$ as

$$\begin{bmatrix} \psi_1 \\ \psi_2 \end{bmatrix} = \begin{bmatrix} \mathrm{e}^{\alpha\lambda_1 x + \frac{1}{4\lambda_1}t + \xi_{10}} \\ \mathrm{e}^{-\left(\alpha\lambda_1 x + \frac{1}{4\lambda_1}t + \xi_{10}\right)} \end{bmatrix},$$

where ξ_{10} is arbitrary constant. Once we let $\lambda_1 = -3/2$, $\alpha = 1/3$, $\xi_{10} = 0$, $g_1(t) = \tanh(3t)$, then we can obtain the single-soliton solutions of the KMM system (3.1) via Theorem 3.1, shown below

$$\begin{aligned} u_{ss}(x,t) &= \frac{4\mathrm{e}^{-x}}{3\mathrm{e}^{-2x-\frac{1}{3}t} + 3\mathrm{e}^{\frac{1}{3}t}}, \\ v_{ss}(x,t) &= \frac{[x + 3\tanh(3t) + 2]\,\mathrm{e}^{-2x-\frac{1}{3}t} + \mathrm{e}^{\frac{1}{3}t}[x + 3\tanh(3t) - 2]}{3\mathrm{e}^{-2x-\frac{1}{3}t} + 3\mathrm{e}^{\frac{1}{3}t}}. \end{aligned} \tag{3.9}$$

3.2. Non-trivial seed solutions: single-soliton solutions

However, once we select a non-trivial seed solutions, the corresponding spectral function cannot be directly given, as the corresponding spectral function is complex and may not be analytically represented at this time. Therefore, in this part, we utilize the powerful solving ability of NNs to numerically simulate the spectral functions corresponding to non-trivial seed solutions. Furthermore, based on the spectral functions obtained from non-trivial seed solutions, we embed the Darboux transformation formulas (3.5)–(3.6) of new solutions into the Darboux transformation part of DT-LPNN to construct new unknown localized wave solutions. Then we force the new solutions satisfy zero curvature equation (2.3) of the Lax pairs (3.2) in the loss function, to ensure that the obtained new solutions are the solutions of the KMM system (3.1). Specifically, we treat the single-soliton solutions (3.9) as non-trivial seed solutions in Darboux transformation Theorem 3.1, and obtain corresponding initial and boundary training points, then utilize DT-LPNN to learn the non-trivial seed solutions, spectral parameter and corresponding spectral function, as well as novel localized wave solutions.

Next the spectral parameter is initialized to $\lambda = 1.5$, while the spectral function is initialized to $\psi_j = 0$ and satisfy the free initial–boundary condition, then we consider the following initial and boundary value conditions of KMM system in spatiotemporal region $[-4,4]\times[-1,1]$:

$$\begin{aligned}
&u(x,t=-1) = u_{\mathrm{ss}}(x,-1),\ v(x,t=-1) = v_{\mathrm{ss}}(x,-1),\ x\in[-4,4],\\
&u(-4,t) = u_{\mathrm{ss}}(-4,t),\ u(4,t) = u_{\mathrm{ss}}(4,t),\\
&v(-4,t) = v_{\mathrm{ss}}(-4,t),\ v(4,t) = v_{\mathrm{ss}}(4,t),\ t\in[-1,1].
\end{aligned} \tag{3.10}$$

After that, by using $N_{\mathrm{c}} = 10000$ collocation points and selecting $N_{\mathrm{ib}} = 500$ initial and boundary points from the initial–boundary conditions (3.10), we succeeded in obtaining data-driven spectral function ψ_j, spectral parameter λ, single-soliton seed solutions u, v, and new localized wave solutions $u_{\mathrm{new}}, v_{\mathrm{new}}$ by means of the DT-LPNN. The network achieve relative L^2 norm error of 1.048773e−03 for the $u(x,t)$ and relative L^2 norm error of 7.619877e−04 for the $v(x,t)$, and the total number of L-BFGS iterations within 4700.7526 s is 7106 times.

Fig. 2 provides the training results arising from the DT-LPNN for the data-driven single-soliton solutions, spectral problem and novel localized wave solutions of the KMM system. In the top panel of Fig. 2(a), the true, learned and error dynamics density plots with corresponding amplitude scale size on the right side for data-driven seed solutions [bright single-soliton] u, v have been exhibited. Meanwhile, in the middle panel of Fig. 2(a), the sectional drawings of the prediction and true seed solutions have been shown at the three distinct moments $t = -0.83, 0, 0.83$, here the aforementioned three distinct moments are displayed by using dashed lines of corresponding colors in the top panel of Fig. 2(a). In the bottom panel of Fig. 2(a), we display the prediction density plots and sectional drawings for the prediction new solutions $u_{\mathrm{new}}, v_{\mathrm{new}}$ [here dark single-soliton u_{new} propagates on variable non-zero background wave]. Fig. 2(b) exhibits the loss function curve figure [panel b1] and spectral parameter λ [panel b2] evolution graph arising from the DT-LPNN with 7106 steps L-BFGS optimizations on the loss function, where learned spectral parameter $\lambda = 0.74149$. The three-dimensional plots with contour map for the data-driven spectral function are depicted in Fig. 2(c1) and (c2). Fig. 2(d1) and (d2) display the three-dimensional plots with contour map for the data-driven seed solutions, while Fig. 2(d3) and (d4) showcase the three-dimensional plots with contour map for the data-driven new solutions. We surprised to find that novel localized wave solutions can be generated through the DT-LPNN, which provide more opportunities for the extension of Darboux transformation theory and the discovery of novel localized wave solutions. From Fig. 2(d), we find that using bright single-soliton solution [observe from the perspective of solution u] as seed solution in DT-LPNN can learn new dark single-soliton solution [observe from the perspective of solution u_{new}] through numerical Darboux transformation, which is a new discovery that has not been reported before.

Moreover, we also applied other types of NNs to solve the KMM system and provided detailed training results in Table 1. From Table 1, owing to the relatively complex Lax pairs information, we can observe that the training effect of LPNN-v1 is poor, while the training error of LPNN-v2 is similar to that of PINN, but the training time is longer, so the overall cost-effectiveness is low. From Table 1, we can intuitively observe that LPNNs and DT-LPNN cannot only solve integrable systems but also solve spectral problem of integrable system and numerically obtain spectral parameter and spectral function, where the spectral function Ψ corresponds to the vector spectral function $\{\psi_1, \psi_2\}$, which are all inaccessible to PINN. Interestingly, after spending a long training time, DT-LPNN achieved the best training results and can generate novel localized wave solutions based on Darboux transformation theory, which is a characteristic that the other three NNs do not possess. From Theorem 3.1 and initial–boundary condition (3.10) of seed solutions, one can know that the new localized wave solutions $u_{\mathrm{new}}, v_{\mathrm{new}}$ are equal to the data-driven bright single-soliton solutions plus a fractional function related to the data-driven spectral parameter and spectral function. Furthermore, from Fig. 2, one can observe that the new localized wave solution u_{new} is a dark soliton solutions on a variable non-zero background wave, which is different from the dark soliton solution u on a zero background plane wave in Ref. [50]. To our best knowledge, the novel data-driven localized wave solutions discovered in this article has not been observed and reported yet, thus we believe that we have generated and discovered a novel data-driven localized wave solution of the KMM system via the DT-LPNN.

3.3. Non-trivial seed solutions: two-soliton solutions

In the previous subsection, we used single-soliton solutions as non-trivial seed solutions and generated novel localized wave solutions via the DT-LPNN, which is a dark soliton solution on a variable non-zero background wave as from the perspective of u_{new}. In this part, we further consider using two-soliton solutions as non-trivial seed solutions, and then apply DT-LPNN to construct new localized wave solutions for the KMM system (3.1). From the Theorem 1 of Ref. [51], one can directly derive the two-soliton solutions by applying N-fold Darboux transformation with parameters $N = 2$, $\alpha = 1/3$, $\theta(t) = \cos(3t)$ and spectral parameters $\lambda_1 = -3/2$, $\lambda_2 = -1$, as follows

$$\begin{aligned}
u_{\mathrm{ts}}(x,t) &= \frac{-20\mathrm{e}^{-\frac{7}{3}x-\frac{1}{2}t} + 30\mathrm{e}^{-\frac{8}{3}x-\frac{1}{3}t} + 30\mathrm{e}^{-\frac{2}{3}x+\frac{1}{3}t} - 20\mathrm{e}^{-x+\frac{1}{2}t}}{75\mathrm{e}^{-\frac{4}{3}x-\frac{1}{6}t} + 75\mathrm{e}^{-2x+\frac{1}{6}t} + 3\mathrm{e}^{-\frac{10}{3}x-\frac{5}{6}t} + 3\mathrm{e}^{\frac{5}{6}t} - 144\mathrm{e}^{-\frac{5}{3}t}},\\
v_{\mathrm{ts}}(x,t) &= \frac{\Upsilon}{75\mathrm{e}^{-\frac{4}{3}x-\frac{1}{6}t} + 75\mathrm{e}^{-2x+\frac{1}{6}t} + 3\mathrm{e}^{-\frac{10}{3}x-\frac{5}{6}t} + 3\mathrm{e}^{\frac{5}{6}t} - 144\mathrm{e}^{-\frac{5}{3}t}},
\end{aligned} \tag{3.11}$$

here

$$\begin{aligned}
\Upsilon =& [x + 3\cos(3t) + 5]\mathrm{e}^{-\frac{10}{3}x-\frac{5}{6}t} + [25x + 75\cos(3t) + 25]\mathrm{e}^{-\frac{4}{3}x-\frac{1}{6}t}\\
&+ [25x + 75\cos(3t) - 25]\mathrm{e}^{-2x+\frac{1}{6}t} + [x + 3\cos(3t) - 5]\mathrm{e}^{\frac{5}{6}t}\\
&- [48x + 144\cos(3t)]\mathrm{e}^{-\frac{5}{3}x}.
\end{aligned}$$

We can observe that the form of two-soliton solutions are quite intricate, so it is very difficult to generate novel localized wave solutions using it as seed solutions. Therefore, if utilizing the DT-LPNN can successfully generate novel localized wave solutions, it can also reflect the effectiveness of our proposed DT-LPNN algorithm.

Next we consider the initial and boundary conditions of KMM system (3.1) with zero damping effect condition when the spatiotemporal variables $\{x,t\}\in[-5,5]\times[-1.5,1.5]$, shown as bellow

$$\begin{aligned}
&u(x,t=-1.5) = u_{\mathrm{ts}}(x,-1.5),\ v(x,t=-1.5) = v_{\mathrm{ts}}(x,-1.5),\ x\in[-5,5],\\
&u(-5,t) = u_{\mathrm{ts}}(-5,t),\ u(5,t) = u_{\mathrm{ts}}(5,t),\\
&v(-5,t) = v_{\mathrm{ts}}(-5,t),\ v(5,t) = v_{\mathrm{ts}}(5,t),\ t\in[-1.5,1.5].
\end{aligned} \tag{3.12}$$

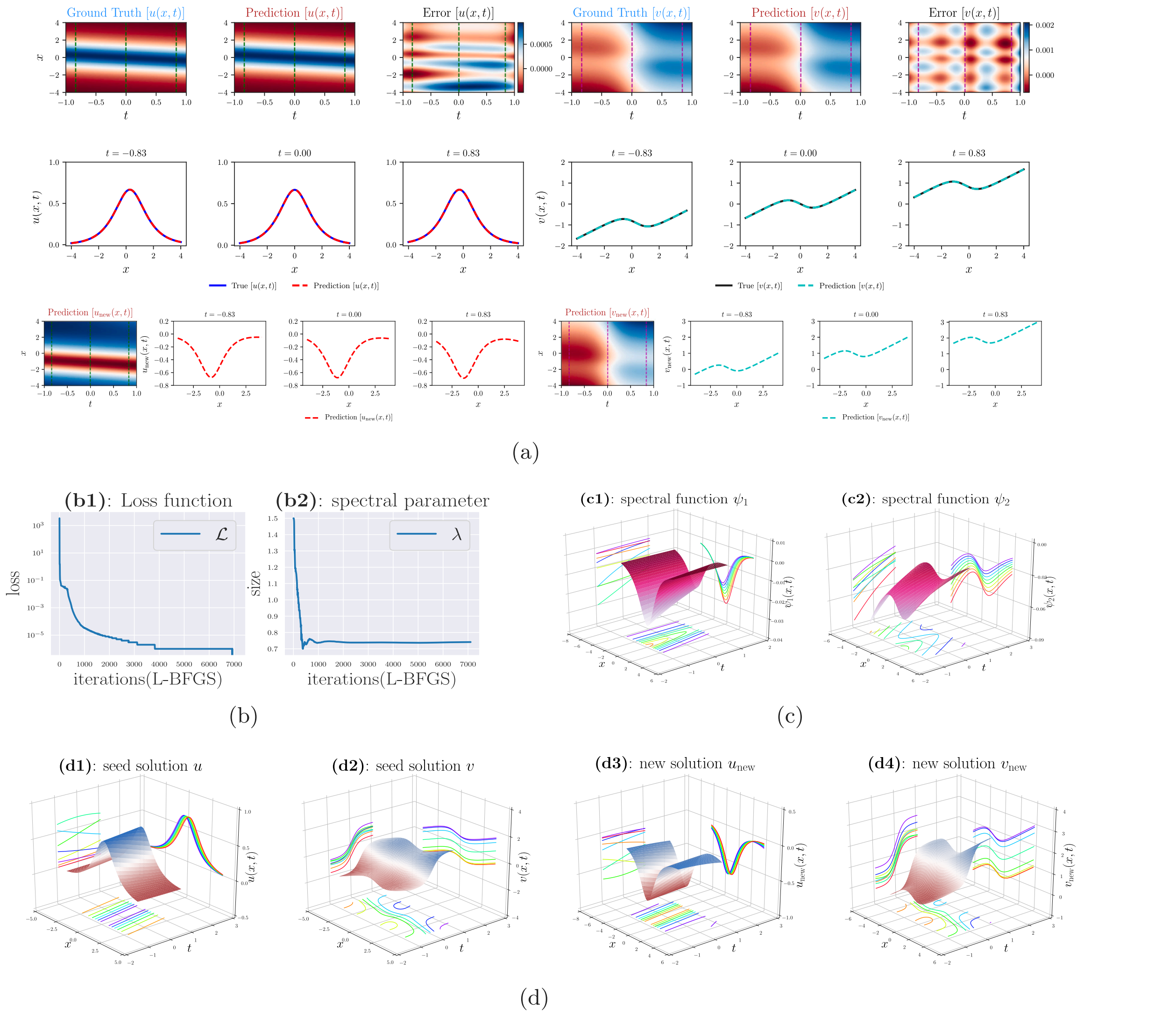

Fig. 2. The training results of single-soliton solutions $u(x,t), v(x,t)$, spectral function $\psi_j(x,t)$ and new localized wave solutions $u_{\rm new}(x,t), v_{\rm new}(x,t)$ for KMM system arising from the DT-LPNN. (a) Top panel: the ground truth, prediction and error dynamics density plots of seed solutions. Middle panel: sectional drawings which contain the true and prediction seed solutions at three distinct moments. Bottom panel: the prediction density plots and sectional drawings of prediction new solutions at three distinct moments; (b) Evolution graph of the loss function [panel b1] and spectral parameter λ [panel b2] in DT-LPNN; (c) The three-dimensional plots with contour map for the data-driven spectral function corresponding to spectral parameter $\lambda = 0.74149$; (d) The three-dimensional plots with contour map for the data-driven seed solutions and new solutions.

Table 1
Performance comparison between DT-LPNN, LPNN-v2, LPNN-v1 and conventional PINN for solving KMM system in Section 3.2.

Networks	$\mathbf{x} \times t$	$\mathcal{D}_{\rm ib}, \mathcal{D}_{\rm c}$	Optimizer	λ	Ψ	L^2 Norm error	Training time	Discovering new solutions
PINN	[−4,4] × [−1,1]	500,10,000	L-BFGS	×	×	u : 2.400451e−03 v : 1.108590e−03	229.2775 s	×
LPNN-v1	[−4,4] × [−1,1]	500,10,000	L-BFGS	0.092695	√	u : 9.495077e−01 v : 3.426840e−01	190.0058 s	×
LPNN-v2	[−4,4] × [−1,1]	500,10,000	L-BFGS	−0.216471	√	u : 3.537780e−03 v : 1.155043e−03	426.5229 s	×
DT-LPNN	[−4,4] × [−1,1]	500,10,000	L-BFGS	0.74149	√	u : 1.048773e−03 v : 7.619877e−04	4700.7526 s	√

We initialize spectral parameter to $\lambda = 0.5$, then we initialize the spectral function to $\psi_j = 0$ and let it satisfy the free initial–boundary condition. By utilizing the initial and boundary conditions (3.12), we choose $N_{\rm ib} = 500$ initial–boundary points and $N_{\rm c} = 20000$ collocation points to generate the training data set for DT-LPNN. We successfully trained and obtained the data-driven two-soliton solutions of the KMM system (3.1) using DT-LPNN, here the relative L^2 norm error of the solution $u(x,t)$ is 2.734971e−03, and the relative L^2 norm error of the solution $v(x,t)$ is 5.493715e−03, the learned spectral parameter is $\lambda =$ 0.700718, and the training time and loss function iteration times of the network are 21160.1722 s and 9118 times, respectively. Moreover, we obtain new localized wave solutions $u_{\rm new}, v_{\rm new}$ for the KMM system via DT-LPNN, which possess unique forms that have never been reported or discovered before.

After utilizing two-soliton solutions as non-trivial seed solutions, we present the vivid numerical results of DT-LPNN for solving the KMM system and generating novel localized wave solutions in Fig. 3. Specifically, we display detailed density plots of the ground truth,

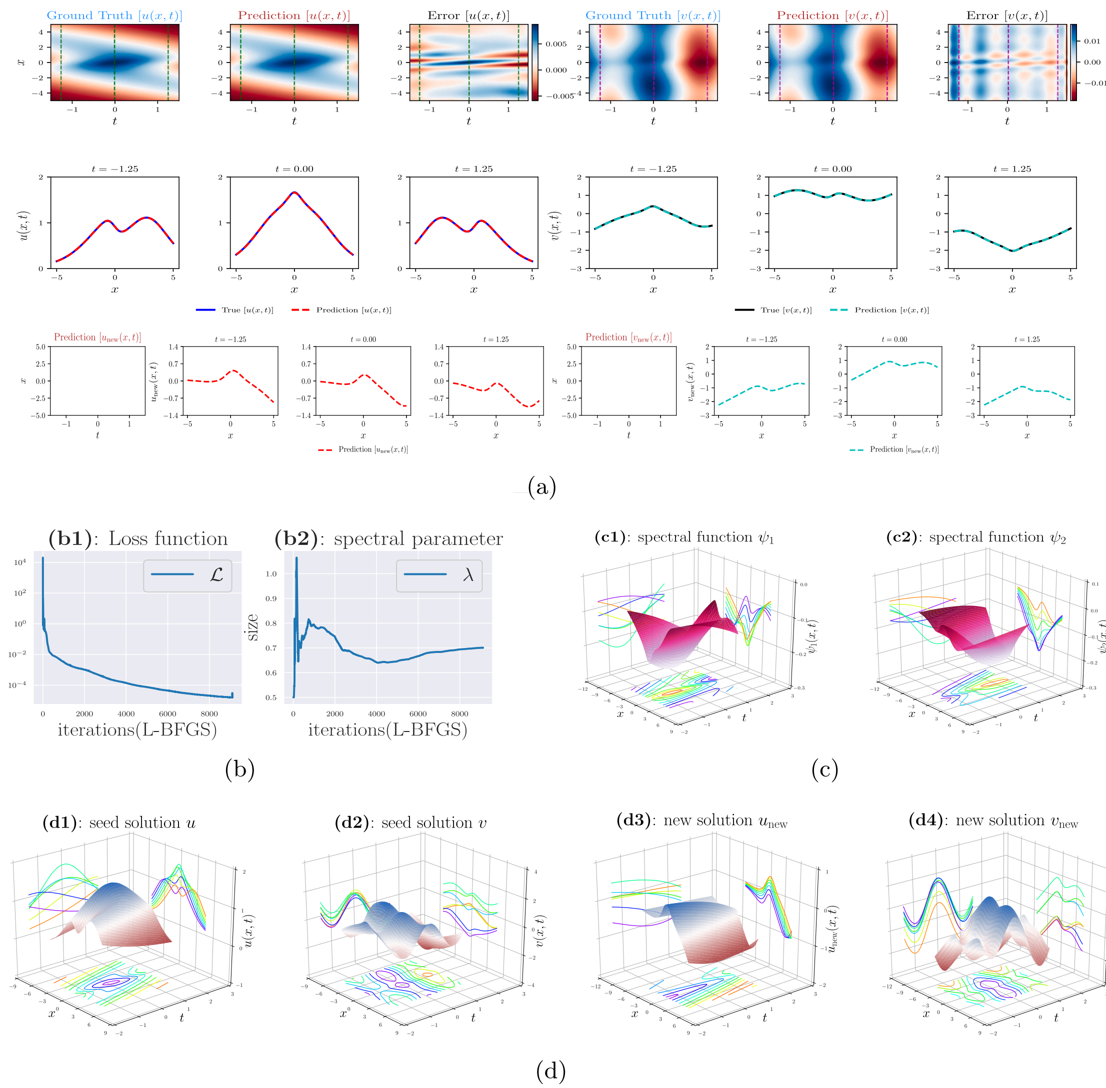

Fig. 3. The training results of two-soliton seed solutions $u(x,t), v(x,t)$, spectral function $\psi_j(x,t)$ and new localized wave solutions $u_{\text{new}}(x,t), v_{\text{new}}(x,t)$ for KMM system arising from the DT-LPNN. (a) Top panel: the ground truth, prediction and error dynamics density plots of seed solutions. Middle panel: sectional drawings which contain the true and prediction seed solutions at three distinct moments. Bottom panel: the prediction density plots and sectional drawings of prediction new solutions at three distinct moments; (b) Evolution graph of the loss function [panel b1] and spectral parameter λ [panel b2] in DT-LPNN; (c) The three-dimensional plots with contour map for the data-driven spectral function corresponding to spectral parameter $\lambda = 0.700718$; (d) The three-dimensional plots with contour map for the data-driven seed solutions and new solutions.

prediction and error dynamics for seed solutions $u(x,t), v(x,t)$ in the top panel of Fig. 3(a), as well as exhibit the sectional drawings at three distinct moments corresponding to the green/purple dashed lines of density plots in the middle panel of Fig. 3(a). Besides that, we showcase the prediction density plots and sectional drawings at three distinct moments for prediction new solutions $u_{\text{new}}(x,t), v_{\text{new}}(x,t)$ in the bottom panel of Fig. 3(a). The evolution graphs of the loss function [panel b1] and spectral parameter λ [panels b2] are revealed in Fig. 3(b). Fig. 3(c1–c2) display the three-dimensional plots with contour map of the data-driven spectral function ψ_j corresponding to spectral parameter $\lambda = 0.700718$. Fig. 3(d1–d2) display three-dimensional plots with contour map for the data-driven seed solutions $u(x,t), v(x,t)$, while Fig. 3(d3–d4) exhibit the three-dimensional plots with contour map for the data-driven new solutions $u_{\text{new}}, v_{\text{new}}$. Moreover, we provide a detailed performance comparison of using four different algorithms to solve the KMM system in Table 2. From Table 2, we can observe that LPNN-v1 has the shortest training time but lower training accuracy, while LPNN-v2 has the highest training accuracy. The training time of the standard PINN algorithm is longer than LPNN-v1 but shorter than LPNN-v2, and the training accuracy is lower than LPNN-v2 but higher than LPNN-v1. However, the three algorithms cannot generate novel localized wave solutions. DT-LPNN can generate novel localized wave solutions after spending longer training time, and the training accuracy can also reach the ideal level.

4. Conclusions

In this work, in order to fully utilize the spectral parameter and corresponding spectral function obtained from our proposed LPNNs, we introduce the Darboux transformation method into LPNN and propose novel DT-LPNN model. The strongest advantage of DT-LPNN is its ability to discover novel localized wave solutions for integrable systems, while also ensuring high training accuracy. As is well known, the Darboux transformation method can iteratively construct N-soliton solutions, breathers, and rogue wave solutions of integrable systems via trivial seed solutions. However, leveraging the advantages of the LPNNs algorithm, our proposed DT-LPNN can start from non-trivial seed solutions and embed the Darboux transformation formula related to the seed solution, spectral parameter and spectral function obtained from the NN part into the Darboux transformation part of DT-LPNN,

Table 2
Performance comparison between DT-LPNN, LPNN-v2, LPNN-v1 and conventional PINN for solving KMM system in Section 3.3.

Networks	$\mathbf{x} \times t$	$\mathcal{D}_{\text{ib}}, \mathcal{D}_{\text{c}}$	Optimizer	λ	Ψ	L^2 Norm error	Training time	Discovering new solutions
PINN	[−5,5] × [−1.5,1.5]	500,20,000	L-BFGS	×	×	u : 2.619494e−03 v : 6.804712e−03	2205.5888 s	×
LPNN-v1	[−5,5] × [−1.5,1.5]	500,20,000	L-BFGS	−0.003843	√	u : 3.236687e−01 v : 2.887497e+00	873.6259 s	×
LPNN-v2	[−5,5] × [−1.5,1.5]	500,20,000	L-BFGS	−0.006139	√	u : 2.416786e−03 v : 4.423797e−03	5225.5579 s	×
DT-LPNN	[−5,5] × [−1.5,1.5]	500,20,000	L-BFGS	0.700718	√	u : 2.734971e−03 v : 5.493715e−03	21,160.1722 s	√

thereby generating novel localized wave solution. Finally, we reconstruct fresh Lax pairs informed part and new loss function, it forces the newly generated solution satisfy the compatibility condition/zero curvature equation of Lax pairs corresponding to the integrable system to ensure the reliability of the new solution.

We apply DT-LPNN to study the KMM system and corresponding Lax pairs, obtaining high-precision data-driven seed solutions, spectral parameter and spectral function, as well as generating novel localized wave solutions. Specifically, we treat the bright single-soliton solutions as non-trivial seed solutions and generate new dark single-soliton solutions on variable non-zero background wave [observe from the perspective of u and u_{new}], which is a novel localized wave solution of the KMM system that has not been reported or discovered. Moreover, we also treat the two-soliton solutions as a non-trivial seed solutions and generate novel localized wave solutions for the KMM system that has not been reported or discovered, which is completely different from the dynamics behaviors of the two-soliton solutions. The numerical results indicate that DT-LPNN cannot only solve integrable systems and spectral problems with high accuracy, but also discover novel localized wave solutions.

Regarding the promotional research of DT-LPNN, we have also attempted to utilize the DT-LPNN to study other integrable systems with Lax pairs. However, for many classic integrable systems, it is difficult to generate novel localized wave solutions, such as the Korteweg–de Vries equation, modified Korteweg–de Vries equation and nonlinear Schrödinger equation in Ref. [33]. The main problems that exist in the research process are:

1. We cannot construct novel localized wave solution successfully because the denominator of the fraction function $\boldsymbol{\Gamma}$ in Darboux transformation Theorem 2.1 is sufficiently small during the iteration of the loss function, resulting in the loss function failing to converge or even deteriorate sharply.

2. We can construct novel localized wave solution successfully, but the new solution is almost identical to the non-trivial seed solution, owing to the very small spectral parameter and spectral function cause the function $\boldsymbol{\Gamma}$ in Darboux transformation Theorem 2.1 to approach 0 sufficiently.

The cause of the above problems may be that it is very difficult to discover novel localized wave solutions for classical integrable systems, or it may be that the non-trivial seed solutions in DT-LPNN are not selected properly, and so on. Nevertheless, once providing suitable integrable models to study, we believe that the DT-LPNN proposed in this article possesses the ability to generate novel localized wave solutions for integrable systems with Lax pairs. In conclusion, this article leverages the advantages of LPNNs based on Lax pairs for spectral problems, and first time combines the core idea of Darboux transformation theory to iteratively generate novel localized wave solutions from a small number of initial and boundary data points, this work has significant research value and application prospects.

CRediT authorship contribution statement

Juncai Pu: Writing – review & editing, Writing – original draft, Software, Methodology, Formal analysis, Conceptualization. **Yong Chen:** Writing – review & editing, Supervision, Project administration.

Declaration of competing interest

The authors declare that they have no known competing financial interests or personal relationships that could have appeared to influence the work reported in this paper.

Data availability

Data will be made available on request.

Acknowledgments

We thank Academician Song Jiang of Chinese Academy of Science for many useful conversations and valuable suggestions. The authors gratefully acknowledge the support of the National Natural Science Foundation of China (No. 12175069 and No. 12235007), Science and Technology Commission of Shanghai Municipality, China (No. 21JC1402500 and No. 22DZ2229014), and Natural Science Foundation of Shanghai, China (No. 23ZR1418100).

References

[1] M. Raissi, P. Perdikaris, G.E. Karniadakis, Physics-informed neural networks: A deep learning framework for solving forward and inverse problems involving nonlinear partial differential equations, J. Comput. Phys. 378 (2019) 686–707.
[2] J. Sirignano, K. Spiliopoulos, DGM: A deep learning algorithm for solving partial differential equations, J. Comput. Phys. 375 (2018) 1339–1364.
[3] W. E, B. Yu, The deep Ritz method: A deep learning-based numerical algorithm for solving variational problems, Commun. Math. Stat. 6 (1) (2018) 1–12.
[4] S.C. Dong, Z.W. Li, Local extreme learning machines and domain decomposition for solving linear and nonlinear partial differential equations, Comput. Methods Appl. Mech. Engrg. 387 (2021) 114129.
[5] S. Jin, Z. Ma, K. Wu, Asymptotic-preserving neural networks for multiscale time-dependent linear transport equations, J. Sci. Comput. 94 (2023) 57.
[6] J.R. Chen, X.R. Chi, W. E, Z.W. Yang, Bridging traditional and machine learning-based algorithms for solving PDEs: the random feature method, J. Mach. Learn. 1 (3) (2022) 268–298.
[7] L. Lu, P.Z. Jin, G.F. Pang, Z.Q. Zhang, G.E. Karniadakis, Learning nonlinear operators via deeponet based on the universal approximation theorem of operators, Nat. Mach. Intell. 3 (3) (2021) 218–229.
[8] H.Y. Li, S. Jiang, W.J. Sun, L.W. Xu, G.Y. Zhou, A model-data asymptotic-preserving neural network method based on micro-macro decomposition for gray radiative transfer equations, Commun. Comput. Phys. 35 (2024) 1155–1193.
[9] A. Scott, Encyclopedia of Nonlinear Science, Routledge Press, London, 2004.
[10] N.J. Zabusky, M.D. Kruskal, Interactions of solitons in a collisionless plasma and the recurrence of initial states, Phys. Rev. Lett. 15 (1965) 240–243.
[11] G.E. Hinton, S. Osindero, Y.W. Teh, A fast learning algorithm for deep belief nets, Neural Comput. 18 (2006) 1527–1554.
[12] I. Goodfellow, Y. Bengio, A. Courville, Deep Learning, MIT Press, Cambridge, 2016.
[13] J. Li, Y. Chen, Solving second-order nonlinear evolution partial differential equations using deep learning, Commun. Theor. Phys. (Beijing) 72 (2020) 105005.
[14] J.C. Pu, J. Li, Y. Chen, Soliton, breather and rogue wave solutions for solving the nonlinear Schrödinger equation using a deep learning method with physical constraints, Chin. Phys. B 30 (2021) 060202.
[15] W.Q. Peng, J.C. Pu, Y. Chen, PINN deep learning for the Chen-Lee-Liu equation: rogue wave on the periodic background, Commun. Nonlinear Sci. Numer. Simul. 105 (2022) 106067.

[16] J.C. Pu, Y. Chen, Data-driven vector localized waves and parameters discovery for Manakov system using deep learning approach, Chaos Solitons Fractals 160 (2022) 112182.
[17] J.C. Pu, Y. Chen, Data-driven forward-inverse problems for Yajima-Oikawa system using deep learning with parameter regularization, Commun. Nonlinear Sci. Numer. Simul. 118 (2023) 107051.
[18] W.Q. Peng, Y. Chen, N-Double poles solutions for nonlocal Hirota equation with nonzero boundary conditions using Riemann-Hilbert method and PINN algorithm, Phys. D 435 (2022) 133274.
[19] J.C. Sun, X.Y. Tang, Y. Chen, Exploring two-dimensional internal waves: A new three-coupled Davey–Stewartson system and physics-informed neural networks with weight assignment methods, Phys. D 459 (2024) 134021.
[20] H.J. Zhou, J.C. Pu, Y. Chen, Data-driven forward-inverse problems for the variable coefficients Hirota equation using deep learning method, Nonlinear Dynam. 111 (2023) 14667–14693.
[21] L. Wang, Z.Y. Yan, Data-driven peakon and periodic peakon solutions and parameter discovery of some nonlinear dispersive equations via deep learning, Phys. D 428 (2021) 133037.
[22] L. Wang, Z.J. Zhou, Z.Y. Yan, Data-driven vortex solitons and parameter discovery of 2D generalized nonlinear Schrödinger equations with a PT-symmetric optical lattice, Comput. Math. Appl. 140 (2023) 17–23.
[23] J. Song, Z.Y. Yan, Deep learning soliton dynamics and complex potentials recognition for 1D and 2D $\mathcal{PT}$-symmetric saturable nonlinear Schrödinger equations, Phys. D 448 (2023) 133729.
[24] J. Song, M. Zhong, G.E. Karniadakis, Z.Y. Yan, Two-stage initial-value iterative physics-informed neural networks for simulating solitary waves of nonlinear wave equations, J. Comput. Phys. 505 (2024) 112917.
[25] Z.J. Zhou, L. Wang, Z.Y. Yan, Data-driven discoveries of Bäcklund transformations and soliton evolution equations via deep neural network learning schemes, Phys. Lett. A 450 (2022) 128373.
[26] J.C. Chen, J. Song, Z.J. Zhou, Z.Y. Yan, Data-driven localized waves and parameter discovery in the massive Thirring model via extended physics-informed neural networks with interface zones, Chaos Solitons Fractals 176 (2023) 114090.
[27] Z.J. Zhou, Z.Y. Yan, Is the neural tangent kernel of PINNs deep learning general partial differential equations always convergent? Phys. D 457 (2024) 133987.
[28] S.F. Sun, S.F. Tian, B. Li, Data-driven high-order rogue waves and parameters discovery for Gardner equation using deep learning approach, Results Phys. 57 (2024) 107386.
[29] X.F. Zhou, C.Z. Qu, W.J. Yan, B. Li, Mastering the Cahn-Hilliard equation and Camassa–Holm equation with cell-average-based neural network method, Nonlinear Dynam. 111 (2023) 4823–4846.
[30] B.W. Zhu, W.B. Bo, Q.H. Cao, K.L. Geng, Y.Y. Wang, C.Q. Dai, PT-symmetric solitons and parameter discovery in self-defocusing saturable nonlinear Schrödinger equation via LrD-PINN, Chaos 33 (2023) 073132.
[31] S.N. Lin, Y. Chen, A two-stage physics-informed neural network method based on conserved quantities and applications in localized wave solutions, J. Comput. Phys. 457 (2022) 111053.
[32] S.N. Lin, Y. Chen, Physics-informed neural network methods based on Miura transformations and discovery of new localized wave solutions, Phys. D 445 (2023) 133629.
[33] J.C. Pu, Y. Chen, Lax pairs informed neural networks solving integrable systems, J. Comput. Phys. 510 (2024) 113090.
[34] V.B. Matveev, M.A. Salle, Darboux Transformations and Solitons, Springer-Verlag, 1991.
[35] G. Darboux, On a proposition relative to linear equations, Paris: C. R. Acad. Sci. 94 (1882) 1456–1459.
[36] B. Birnir, H.P. McKean, A. Weinstein, The rigidity of sine-Gordon breathers, Comm. Pure Appl. Math. 47 (1994) 1043–1051.
[37] L. Draper, Freak ocean waves, Weather 21 (1966) 2–4.
[38] R. Camassa, D. Holm, An integrable shallow water equation with peaked solitons, Phys. Rev. Lett. 71 (1993) 1661–1664.
[39] J. Satsuma, M.J. Ablowitz, Two-dimensional lumps in nonlinear dispersive systems, J. Math. Phys. 20 (1979) 1496–1503.
[40] C.S. Gardner, J.M. Greene, M.D. Kruskal, R.M. Miura, Method for solving the Korteweg–de Vries equation, Phys. Rev. Lett. 19 (19) (1967) 1095–1097.
[41] R. Hirota, Direct Methods in Soliton Theory, Springer-verlag, Berlin, 2004.
[42] H.D. Wahlquist, F.B. Estabrook, Bäcklund transformation for solutions of the Korteweg–de Vries equation, Phys. Rev. Lett. 31 (23) (1973) 1386.
[43] K. Hornik, M. Stinchcombe, H. White, Multilayer feedforward networks are universal approximators, Neural Netw. 2 (5) (1989) 359–366.
[44] A.P. Fordy, J. Gibbons, Factorization of operators I. Miura transformations, J. Math. Phys. 21 (1980) 2508–2510.
[45] M. Stein, Large sample properties of simulations using Latin hypercube sampling, Technometrics 29 (2) (1987) 143–151.
[46] R.A. Kraenkel, M.A. Manna, V.V. Merle, Nonlinear short-wave propagation in ferrites, Phys. Rev. E 61 (1) (2000) 976–979.
[47] F.T. Nguepjouo, V.K. Kuetche, T.C. Kofane, Soliton interactions between multivalued localized waveguide channels within ferrites, Phys. Rev. E 89 (2014) 063201.
[48] V.K. Kuetche, F.T. Nguepjouo, T.C. Kofane, Engineering magnetic polariton system with distributed coefficients: Applications to soliton management, Chaos Solitons Fractals 66 (2014) 17–30.
[49] H.T. Tchokouansi, V.K. Kuetche, T.C. Kofane, On the propagation of solitons in ferrites: The inverse scattering approach, Chaos Solitons Fractals 86 (2016) 64–74.
[50] Y.L. Ma, B.Q. Li, Kraenkel-Manna-Merle saturated ferromagnetic system: Darboux transformation and loop-like soliton excitations, Chaos Solitons Fractals 159 (2022) 112179.
[51] Y. Shen, B. Tian, T.Y. Zhou, X.T. Gao, N-Fold Darboux transformation and solitonic interactions for the Kraenkel-Manna-Merle system in a saturated ferromagnetic material, Nonlinear Dynam. 111 (2023) 2641–2649.